



30 precious material and making all effort to recover copper otherwise lost in slag. This find will  
31 potentially shed new light on a range of important issues of Shang archaeology, including the  
32 regional variation of Shang metallurgical styles and the provenance of copper in the Shang  
33 period. This research also encourages researchers to look into archaeological soil samples with  
34 abnormally high copper content and understand the particles in them causing these high  
35 readings.

36

### 37 **Key words**

38 Micro-slag, bronze casting workshop, in-situ analysis, microscopic analysis, refining

39

### 40 **1. Introduction**

41 Metal smelting and processing in the pre-modern period generated a range of material  
42 remains such as slag, metal spillage, crucible/furnace fragments, tuyères and casting moulds.  
43 The detailed analysis of these remains can provide crucial information about ancient  
44 metallurgical technology and facilitate the study of function and spatial organization of metal  
45 workshops. Many authors have published research on the scientific characterization of metal  
46 processing remains (e.g. Rovira, 2002, Rehren, 2003, Hauptmann, 2014, Liu, et al., 2015,  
47 Murillo-Barroso, et al., 2017, Rademakers and Farci, 2018). However, little attention has  
48 previously been paid to the sample collection strategy (but see Rademakers and Rehren, 2016).  
49 It has been known that metal smelting at the dawn of metallurgy may leave little material  
50 evidence due to the high purity of raw materials and relatively small production scale (Craddock,  
51 2000, O'Brien, 2004, Radivojevic, et al., 2010). Additionally, workers may sometimes further  
52 process smelting slag for embedded metallic inclusions. In sharp contrast to the massive slag  
53 mounds in many Late Bronze Age sites, a range of Chalcolithic and Early Bronze Age sites  
54 only revealed nut-sized or smaller slag fragments (less than 1 cm), which are believed to be  
55 intentionally crushed after smelting in order to retrieve metallic prills trapped in them (Epstein,  
56 1993, Montero-Ruiz, 1993, Golden, et al., 2001, Shugar, 2003, Bourgarit, 2007, Burger, et al.,  
57 2010). To recover these micro-slags in the field, a careful sample collection strategy involving  
58 geochemical survey and wet-sieving of soil samples is needed during the excavation.

59 This article demonstrates that it is equally important to investigate micro-slag from bronze

60 casting workshops, using as a case study a Middle-Shang period (14<sup>th</sup>-13<sup>th</sup> century BC) bronze  
61 casting workshop at Taijiashi in Anhui province, China. The systematic analysis of various types  
62 of metallurgical remains created a significantly more comprehensive view of bronze processing  
63 activities at this important settlement in Central China than would have been otherwise possible.

64

### 65 1.1 Archaeological Background

66 The site of Taijiashi is located at Funan county, northwestern Anhui province, more than  
67 500 km away from the Shang capitals in the Central Plains, and about 200-300 km from the  
68 copper belt in the Yangtze River valley (Figure 1). The site is at the north bank of the Runhe  
69 River (润河), a branch of the Huaihe River (淮河). In the 1930s to 1950s, a number of important  
70 Shang bronze ritual vessels had been discovered as chance finds in the old course of the Runhe  
71 River (Ge, 1959), indicating the residence of Shang elites in this area. However, it had not been  
72 clear whether these ritual artefacts were locally produced or imported from the Central Plains.  
73 Since 2014, the site of Taijiashi was excavated by a joint archaeological team of Anhui Provincial  
74 Institute of Archaeology and Wuhan University. The site consists of five mounds. The largest  
75 one is around 4000 m<sup>2</sup>, surrounded by a moat about 10 m wide. The mound was mostly  
76 excavated and revealed rich material remains demonstrating Shang people lived at this site and  
77 conducted metallurgical craft-production.

78

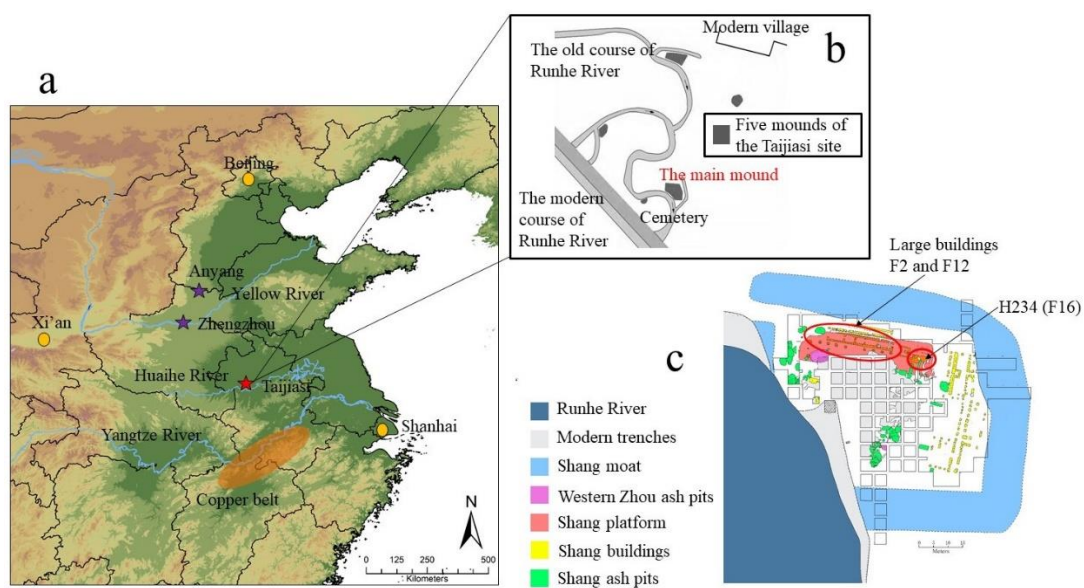


Figure 1 The site of Taijiashi. The geographic distance between the Taijiashi site and Shang capitals in the north is shown in (a). Its five mounds are shown in dark grey colour in (b). (c)

is the plan of the Taijiashi major mound. The metallurgical workshop H234 is located on the same platform as the large buildings F2 and F12.

79

80 Based on stratigraphic association and pottery typology, the Shang occupation of this site  
81 is divided into two phases. The first phase is from the Upper Erligang to the Early Huanbei  
82 Period (Middle Shang I-II). The second one is dated to the later Huanbei period or Yinxu I stage  
83 (Middle Shang III) (see Table 1 for a chronological framework of the Middle Shang). Three  
84 seasons of excavations revealed many important features including 16 building foundations and  
85 262 ash pits, which mostly dated to the later period of this site. To the west of this mound, 7  
86 tombs of the second phase were excavated, revealing a number of ritual bronze vessels and jade  
87 objects. A rammed earth platform was identified in the northern part of the main mound with  
88 four buildings (F2, F12, F14, F16) on it. The rammed earth platform is arguably a strategic  
89 feature of the site and its current surface is still about 1m above the ground. Both F2 and F12  
90 were large long houses with a significant size (over 20m in length), and are thought to be elite  
91 residence or ritual places, due to their size and special location (He and Gong, 2018).

92

93 Table 1 Chronological table of the Middle Shang period and its major sites

Period	Date	Major sites
Middle Shang I	c. 1400-1350 BC	Xiaoshuangqiao site
Middle Shang II	c. 1350-1300 BC	Huanbei Shang City
Middle Shang III	c. 1300-1250 BC	Huanbei Shang City

94

95 The most prominent craft production at this site was bronze casting, indicated by a great  
96 number of metallurgical remains such as slag, furnace/crucible fragments, and moulds that were  
97 found in the moat and ash pits. The majority of them were dated to the later stage of the site  
98 (13<sup>th</sup> century BC). This article focuses on this period while the remains found in the earlier  
99 contexts suggest there was already metallurgical production taking place then. The mould  
100 fragments of Taijiashi suggest that ritual vessels were the major products of the site (He and  
101 Gong, 2018). It is the first Shang period bronze casting workshop identified in the Huaihe River  
102 valley, demonstrating that the production of ritual vessels was not confined to the capital sites

103 in the Central Plain.

104 Bronze casting remains of the later stage were found in three types of contexts. The first  
105 one is the foundations of buildings, where the metallurgical remains were likely introduced  
106 accidentally during the construction process. The majority of metallurgical remains were found  
107 in ash pits and the moat, the second context type. More than 30 ash pits revealed slag,  
108 crucible/furnace fragments and/or mould pieces. Two trial trenches in the east part of the moat  
109 also yielded many slags in the sediment. Metallurgical remains found in this context type were  
110 most likely waste dumped during the production, or secondary deposits formed after the  
111 production. The third context type is the fill of building F16 on the rammed earth platform. It  
112 has an area of approximately 48m<sup>2</sup> with two sectors H234 and H241; metallurgical remains  
113 were mainly found in sector H234. Remains of other crafts (such as bone tool manufacturing  
114 or pottery making) were absent from this context. The wall foundation was not found but 26  
115 column bases around this building indicate it was roofed. It was dated to the later phase of this  
116 site based on pottery sherds recovered from the fill of this feature. The excavation revealed its  
117 first locus containing mainly podzolic sediment, in which green and black particles (< 1 cm)  
118 were found embedded. There were, however, only one copper fragment (H234①:5) and a few  
119 pieces of moulds, slag and crucible/furnace fragments revealed during the initial excavation.

120 An investigation of Shang metallurgical activities at this site was conducted jointly by the  
121 Institute for Cultural Heritage and History of Science & Technology (ICHHST), University of  
122 Science and Technology Beijing (USTB), the School of History, Wuhan University and School  
123 of Archaeology and Museology, Peking University. An innovative sampling strategy was  
124 employed to collect not only macro-metallurgical remains but also soil samples from  
125 geochemically abnormal strata and units. These samples were processed by wet-sieving to  
126 retrieve micro-artefacts, which were then subjected to detailed lab-based analyses leading to  
127 much new information concerning the nature of metallurgical activities at this site.

128

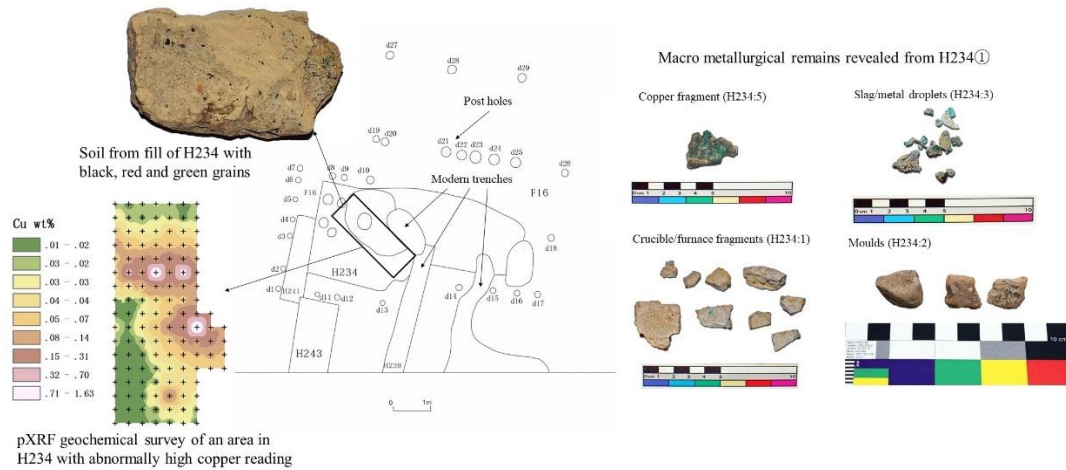


Figure 2 Plan of F16 and metallurgical remains including slag, crucible, and mould fragments found in sector H234. The northwestern corner of H234 shows elevated Cu and Ca reading during pXRF survey. The fill of this part contains many black, red and green particles.

129

## 130 2. Methodology

131 A Thermofisher Niton XL3t pXRF was used to conducted systematic in-situ soil analyses at  
 132 the site. Soil mode was used and the collection time was 90 s. Profile soil samples from H234  
 133 were collected and analysed with X-ray powder diffraction (XRD) and Fourier Transformed  
 134 Infrared (FTIR) spectrometry to study their mineralogical composition and thermal history. A  
 135 Rigaku D/max-rb X-ray diffractometer with Cu-K $\alpha$  radiation and an operating voltage of 30-  
 136 45 kV was used for XRD analysis. FTIR measurements were performed with a Thermofisher  
 137 IS5 spectrometer in transmission mode. Soil samples were collected for floatation and wet-  
 138 sieving from the area with abnormally high Cu content identified by in-situ pXRF analysis. The  
 139 heavy fraction of the samples was wet-sieved with an 80 mesh sieve to recover fine remains.  
 140 This was followed by a careful examination under the stereo-microscope, picking out fragments  
 141 with features of copper processing remains (e.g. green/black colour, porous/glassy texture,  
 142 metallic lustre). The soil samples were obtained from ash pits, the moat and sector H234. In  
 143 total, 161.5 litre of soil were treated by this method.

144 Macro-metallurgical samples, including slag, crucible, and metal fragments as well as micro-  
 145 artefacts were subjected to detailed characterization at the archaeometry lab of ICHHST, USTB.  
 146 Optical microscopy and a Tescan Vega III SEM equipped with a Bruker XFLASH 6|10 energy  
 147 dispersive spectrometer (EDS) was used to investigate the microstructure and chemical  
 148 composition of soil, slag and metal samples. The accelerating voltage was set to 20 kV and the

149 live collecting duration was 60 s. Bulk compositions of micro-slags were determined by  
150 analysing the area of a polygon fitted into the slag fragment, including all metal prills and  
151 residual mineral inclusions. The data quality of the instrument was monitored with glass  
152 (Corning B) and tin bronze standards (CHARM set).

153

### 154 3. Results

#### 155 3.1. Metallurgical activity at Taijiasi

156 Workshop H234

157 Macro metallurgical remains from H234 were analyzed for their chemical composition and  
158 microscopic structure. The copper fragment H234①:5 was identified as a piece of pure copper  
159 with impurities of less than 1 wt%. The crucible/furnace fragments (H234①:1) are associated  
160 with alloying and casting processes with abundant bronze prills, tin oxide and copper oxide in  
161 them (Figure 3).

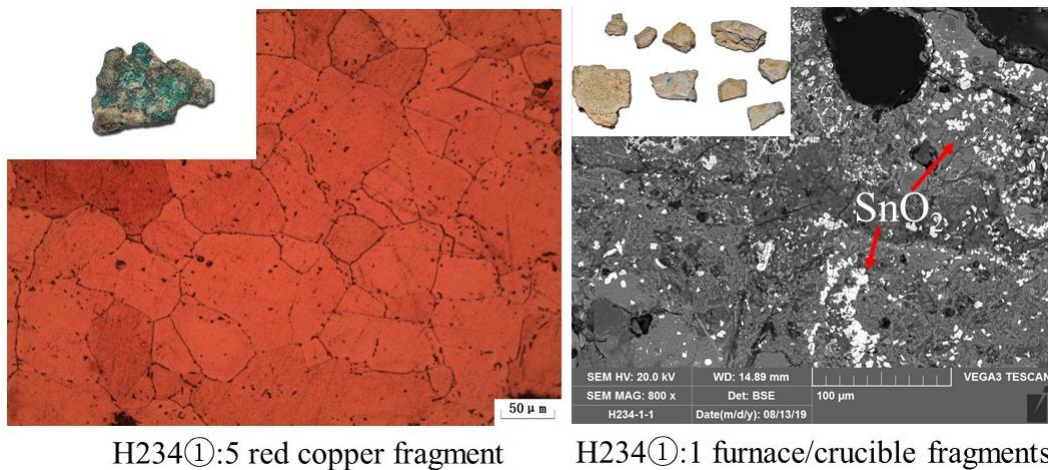


Figure 3 Microscopic images of the H234 ① :5 copper fragment and H234 ① :1 furnace/crucible fragments. H234①:5 has a typical metallographic structure of pure copper with  $\alpha$  grains and Cu-Cu<sub>2</sub>O eutectic structure. H234①:1 contains many SnO<sub>2</sub> particles in its slag lining.

162

163 The sampling interval of the in-situ geochemical survey was first set to 50 cm, and 80 points  
164 in total were analysed. A small area in the northwestern corner of sector H234 shows  
165 significantly elevated Cu and Ca contents. A more focused survey with a sample interval of 10  
166 cm was then conducted in this area. The result shows that most Cu and Ca abnormal points  
167 concentrate in an irregular area of this part.



168 A modern trench cutting through the central part of the building exposed a profile of six loci  
 169 (Figure 4). Locus 1 (H234①) is the podzolic soil with green and black inclusions. Locus 2  
 170 (H234②) is a hard greyish-whitish material. Loci 3-4 (H234③, H234④) are clay-rich yellow  
 171 soil. Locus 5 (H234⑤) is podzolic soil containing ash and charcoal fragments. Level 6 (H234⑥)  
 172 is the natural soil beneath the foundation of building F16.  
 173

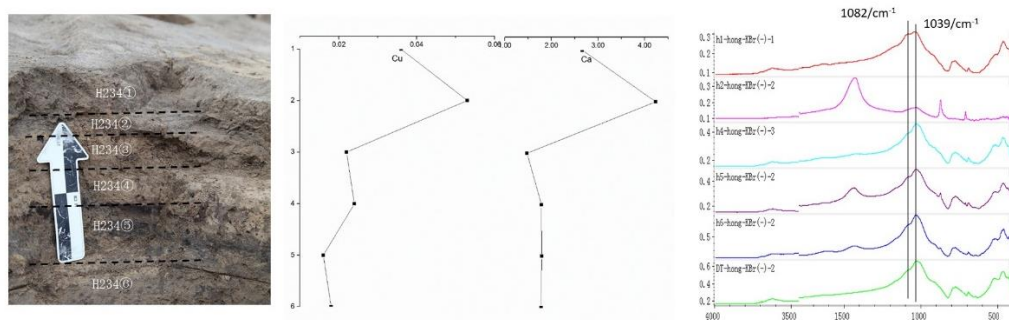


Figure 4 Profile of Cu and Ca rich area in H234. In-situ pXRF analysis shows that H234①-② are rich in Cu and Ca. FTIR analysis shows H234① has an additional absorption band around 1080/cm<sup>-1</sup> and H234② has a strong absorption band around 1470/cm<sup>-1</sup>.

174

175 The microscopic analyses show that H234③-⑥ are loess-like soil. H234① is also loess-like  
 176 but contains much higher Cu and Ca than H234③-⑥. Its IR spectrum shows a stronger  
 177 absorption band around 1082/cm<sup>-1</sup>. According to previous FTIR investigation of archaeological  
 178 sediments (Berna, et al., 2007), the major absorption band of fired clay tends to move from  
 179 1030/cm<sup>-1</sup> to 1080/cm<sup>-1</sup>. It is therefore suggested that H234① contains more fired clay than  
 180 H234③-⑥. H234② is chemically and mineralogically different from the rest of the samples.  
 181 Chemical analysis with SEM-EDS shows it contains mainly CaO with a small amount of silica.  
 182 Its IR spectrum shows a strong absorption band around 1470/cm<sup>-1</sup>, corresponding with  
 183 carbonate minerals (Monnier, 2018). XRD analysis proves H234② contains mainly calcite  
 184 (CaCO<sub>3</sub>) as well as a small amount of quartz (SiO<sub>2</sub>) and albite (NaAlSi<sub>3</sub>O<sub>8</sub>) (Figure S2). It was  
 185 probably a lime-lined floor of this workshop. Its surface has a high Cu content, demonstrating  
 186 the metallurgical activities that took place on it.



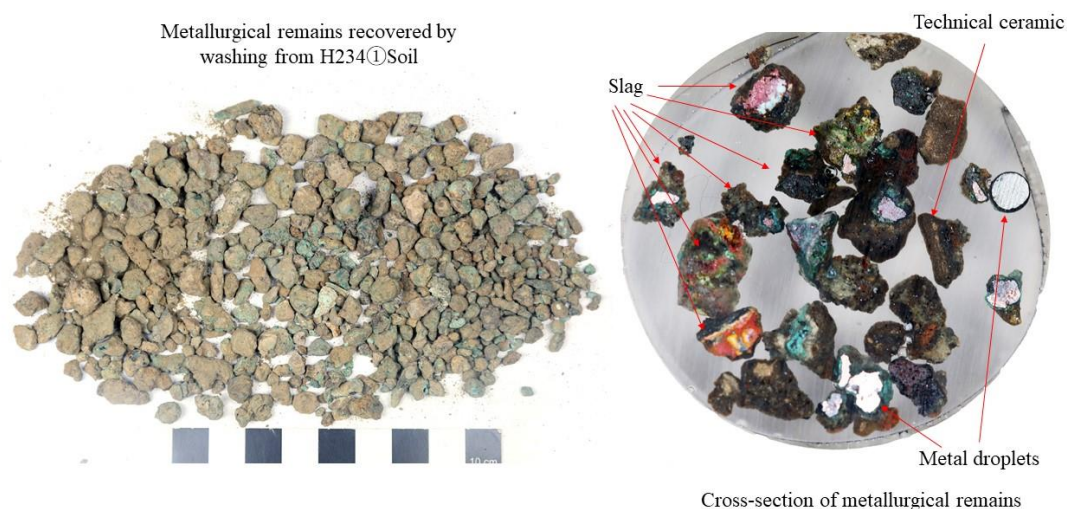


Figure 5 Micro-artefacts recovered from the H234① soil samples. The diameter of the resin block is 3 cm. Many of the fragments in the left picture are conglomerates of many slag pieces, bound by clay matrix. The actual particle size of slag can only be measured by microscopic analysis.

187

188        Though there was only a limited quantity of macro-metallurgical remains from  
 189 H234①, wet-sieving of soil samples revealed many microscopic remains. The heavy portion  
 190 mounted in epoxy resin was examined by OM and SEM. A considerable number of slag  
 191 fragments and metal prills were identified in these polished blocks. Many of them were still  
 192 coated with a clay shell or embedded in clay matrix, and could not have been identified without  
 193 microscopic examination in cross-sections. The diameters of slag pieces were measured in SEM  
 194 images and their chemical compositions were analysed using SEM-EDS. Among 84 fragments  
 195 randomly selected for analysis, the average particle size is 1210  $\mu\text{m}$ , with a considerable number  
 196 of them below 1000  $\mu\text{m}$  (Table S1, Table S2). Microscopic examination shows they are mostly  
 197 slag fragments and metal prills, while technical ceramic is also occasionally identified (Figure  
 198 6).

199

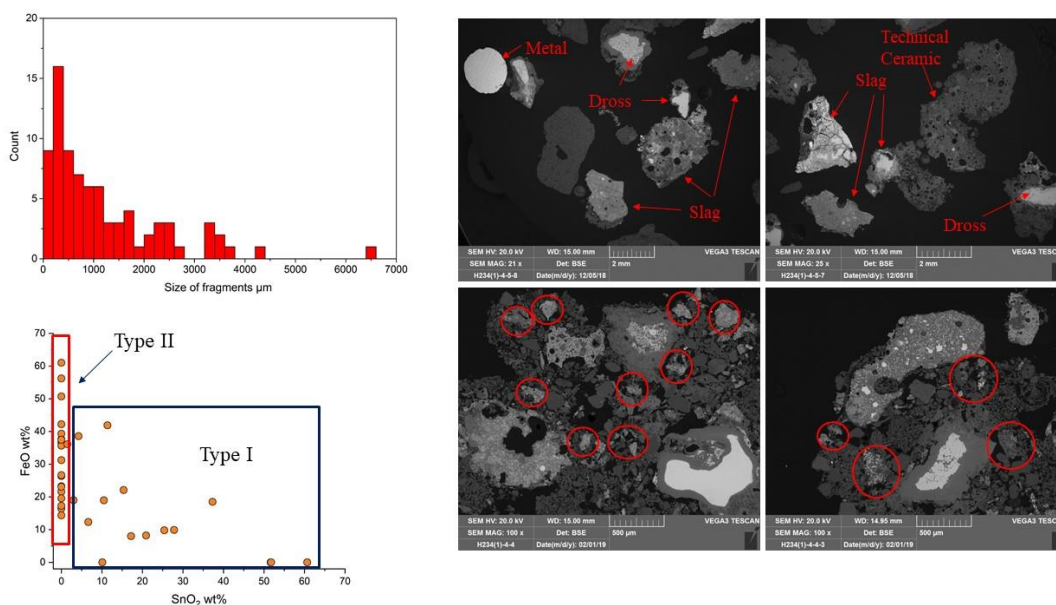


Figure 6 Size distribution and chemical composition of metallurgical remains found in H234① soil samples. Images are microscopic photographs of metallurgical remains. Two images at the lower row show many small slag fragments (labelled by red circles) embedded in the soil matrix. All analysed samples can be divided into two groups (Type I and Type II) on the basis of their tin content.

200

201 Two chemical groups were identified in these samples (Figure 6, Table S1, Table S2). Type  
 202 I remains, including slag, dross and metal prills, are characterized by their high SnO<sub>2</sub> content  
 203 (23.9 wt%) in average. Typically, these fragments are dominated by diamond and needle shaped  
 204 tin oxide, cuprite and sometimes malayaite crystals. These Sn-rich phases are usually associated  
 205 with metallic copper globules with varied Sn content (0-52 wt%). Free-standing bronze prills  
 206 found in polished blocks typically have a spherical morphology. Other alloying elements such  
 207 as As, Sb and Pb were found to be below the detection limit (c. 0.1 wt%) in Type I samples,  
 208 suggesting the final product was tin bronze. Many dross fragments were arguably associated  
 209 with high temperature metal ‘burning’ processes, that is the oxidation of metal at high  
 210 temperatures during working, indicated by the presence of a relatively large metal core and  
 211 diamond shaped tin oxide in the matrix (Figure 7:a,e). On the other hand, extraordinarily high-  
 212 tin globules (>40 wt% Sn) (Figure 7:b and f) suggest fresh tin-rich raw materials such as metallic  
 213 tin or cassiterite were involved in an active alloying process (Rehren 2001; Rovira, 2002, Liu,  
 214 et al., 2015, Rademakers and Farci, 2018). Rounded metal prills might have spilled out from  
 215 crucibles and moulds during melting and casting.

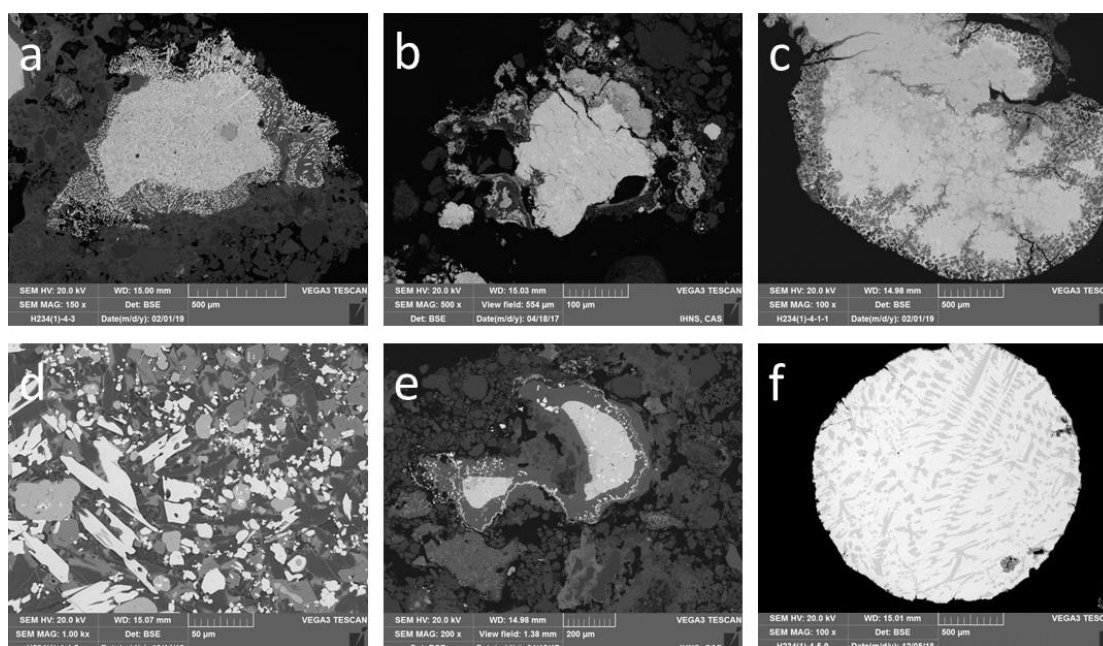


Figure 7 Micrographs of Type I slag, dross and metal prills. a,e: Typical burnt metal with a large metal core surrounded by tin oxides. d: matrix of Type I slag with many tin oxide and copper oxide crystals. b,c,f: Metallic prills/fragments with varied tin content.

216

217 In contrast, Type II remains contain no tin (Sn below detection limit); they account for c.  
 218 70% of the analysed fragments (Figure 6). They are mostly slag fragments, while their CuO and  
 219 FeO contents are highly varied and have a general negative correlation with each other (Figure  
 220 8; note that any metallic copper prills in these fragments were included in the bulk analyses,  
 221 expressed in the total as CuO). This type might be further separated into two subgroups based  
 222 on their CuO and FeO contents. A tentative line could be drawn between a copper-rich (Type  
 223 II-a) (CuO > 40 wt%, FeO < 10 wt%) and an iron-rich group (CuO < 30 wt%, FeO > 10 wt%)  
 224 (Type II-b). The iron-rich slag fragments can have as much as 60 wt% FeO and are dominated  
 225 by angular magnetite ( $\text{Fe}_3\text{O}_4$ ) crystals and sometimes even wüstite (FeO), while the iron-poor  
 226 and copper-rich ones contain mostly globular and dendritic cuprite (Figure 8). Delafossite lathes  
 227 were frequently identified in slag with intermediate CuO and FeO contents (Figure 8). However,  
 228 it has to be borne in mind that these slag particles are generally below 3 mm in size and the  
 229 chemical separation between the two subgroups might be attributed to the varied metallurgical  
 230 practices or highly varied nature of early bronze processing slag (Müller, et al., 2004,  
 231 Rademakers and Rehren, 2016). There are also generally a few percent of CaO,  $\text{K}_2\text{O}$  and  $\text{P}_2\text{O}_5$ ,  
 232 which were likely from fuel ash. The  $\text{SiO}_2/\text{Al}_2\text{O}_3$  ratio of these samples varied between c. 3-4

233 and c. 10-13 with an average of 6.8, while the value of technical ceramics from this site are  
 234 generally 5-6. It indicates that the major source of SiO<sub>2</sub> and Al<sub>2</sub>O<sub>3</sub> in the slag particles was likely  
 235 technical ceramics. A few relatively large slag fragments contain unreacted quartz, which could  
 236 be either residual material from technical ceramics or added flux (Figure 9).

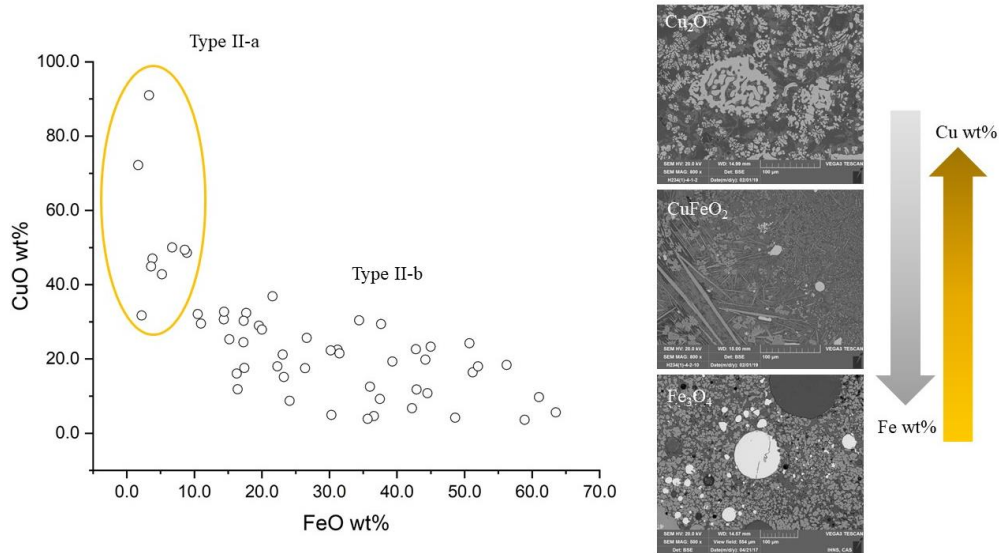


Figure 8 Chemical and mineralogical composition of Type II slag samples. Their typical microstructure changes along with Fe and Cu content. Type II-a slag are rich in Cu but poor in Fe. Type II-b slag are rich in Fe.

237

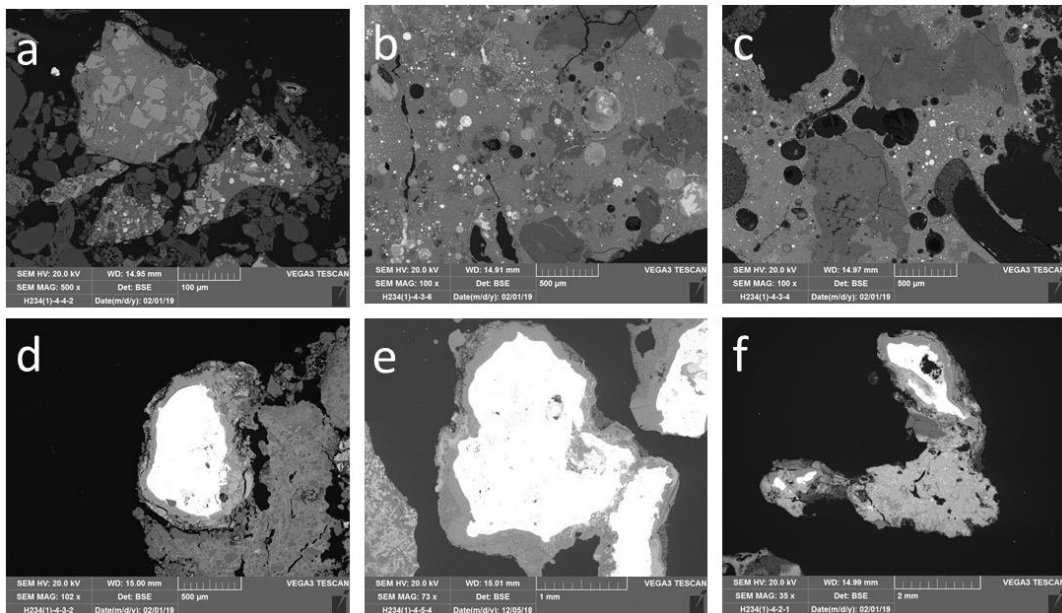


Figure 9 Micrographs of Type II slag. a: slag fragments with angular magnetite crystals. b, c: relatively large slag fragments containing unreacted quartz particles. d, e, f: metallic prills embedded in Type II slag.

238

239 Metallic prills embedded in Type II slag are all identified as non-alloyed copper with a few  
240 percent of Fe as impurity (average 1.5 wt%, see Table S3 for full dataset). The relatively large  
241 (>500  $\mu\text{m}$ ) metal prills usually have an irregular shape and are generally Fe free. They have the  
242 typical Cu-Cu<sub>2</sub>O eutectic structure of pure copper and are either free-standing or combined with  
243 slag pieces (Figure 9).

244

### 245 **3.2. Metallurgical remains from other contexts**

246 Apart from H234, slag, dross, metal fragments and technical ceramics dated to the same  
247 period were also recovered from the foundation of building F12, F14 and F18, the ash pits  
248 located all over the mound, and the sediment in the moat surrounding the mound. Most of these  
249 samples are significantly larger than those found in H234. Wet-sieved soil samples did not  
250 reveal micro-slag fragments like those from H234 ① from any of these contexts in a  
251 considerable quantity. Nineteen slag and crucible/furnace lining samples, and five metal  
252 artefacts/fragment samples were selected for analysis (Table S3, Table S4). Fifteen of the slag  
253 samples contain abundant tin oxide crystals and tin bronze prills. The technical ceramic sample  
254 H291:3-2 does not have developed slag lining but the bronze prills trapped in its interior surface  
255 indicate it was associated with tin bronze processing. The other four samples have high CuO  
256 content (15-57 wt%) but no Sn. One slag sample recovered from the foundation of building F18  
257 (F18JC:5) shows significant FeO content (18.8 wt%) and bears many iron-rich phases such as  
258 rounded wüstite and angular magnetite (Figure 10:e). The remaining three samples are all rich  
259 in CuO and relatively poor in FeO (<10 wt%), similar to Type II-a slag from H234①. Five  
260 artefacts including one arrow head (F15JC:1) and four metal fragments (H291:1, G1③:3-2,  
261 H323:2) were found to be tin bronze (Sn 4.5-19.0 wt%) and only the H321:4 bronze fragment  
262 contains 3.6 wt% Pb. All five samples have an as-cast metallographic structure and show no  
263 signs of hot or cold working.



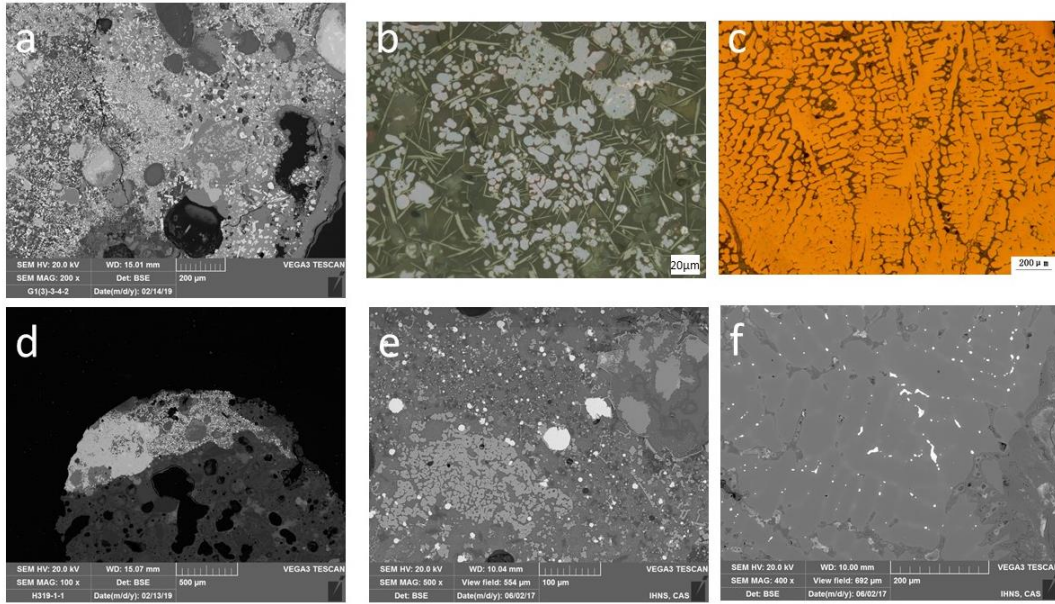


Figure 10 Micrographs of samples from contexts other than H234. a: much tin oxide in slag matrix of G1③:4. b: matrix of H311②:1. Needle-like crystals are delafossite while pale rounded ones are cuprite. c: as-cast metallographic structure of bronze fragment H291:2. d: slag lining of H319:1. e: F18JC:5 slag matrix with much wüstite, magnetite and pure copper prills in it. f: BSE image of H321:4. Lead particles in as-cast bronze structure.

264

265 The scatter plot of Figure 11 shows the comparison between slag of H234① and other  
 266 contexts. A general observation is that samples from these contexts have lower FeO content  
 267 than those from H234①. The Sn-bearing slag from these contexts have similar SnO<sub>2</sub> content  
 268 but the relatively iron-rich ones found in H234① (indicated by dashed oval in Figure 11) were  
 269 not identified elsewhere. Apart from F18JC:5, the Sn-free slag fragments of these contexts also  
 270 have relatively low FeO content, corresponding to Type II-a slag of H234①. F18JC:5 shows  
 271 similar chemical and mineralogical compositions to the Type II-b slag of H234①.

272

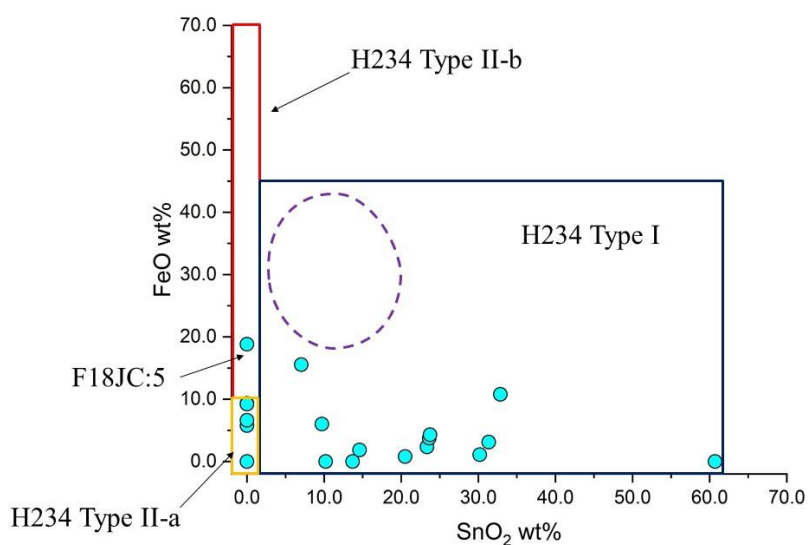


Figure 11 Chemical composition of slag samples from other contexts. The compositional range of H234 Type I and Type II slags are indicated with blue and red / yellow rectangles, respectively.

273

## 274 4. Discussion

### 275 4.1. The metallurgical nature of Taijiasi slag

276 The three main metallurgical processes in an ancient bronze casting workshop are  
 277 alloying/casting, copper melting, and copper refining, particularly for the removal of iron from  
 278 raw copper, while copper smelting could also be conducted at certain contexts. The tin-rich  
 279 Type I slag can be safely associated with the bronze alloying/casting process. The  
 280 extraordinarily high-tin prills indicate that metallic tin or tin oxide was freshly added to the  
 281 melt. The interpretation of the Type II slag and prills is more complicated since copper melting,  
 282 smelting and refining processes can all generate iron- and copper-rich slag free from alloying  
 283 elements. During melting, metallic copper can turn into cuprite due to poorly controlled redox  
 284 conditions, and form delafossite if the metal contained iron, as often is the case for raw copper.  
 285 It is argued the relatively copper-rich but iron-poor slag fragments found in both H234① (Type  
 286 II-a) and other contexts were more likely associated with copper melting practice. The pure  
 287 copper fragment found in H234① (H234①:5) was likely the outcome of such an operation and  
 288 lost during the remelting/alloying process.

289 A refining process in which iron and other impurities in copper were oxidized would  
 290 generate slag with much iron oxide (e.g. magnetite, wüstite) as well as some copper oxides,



291 differentiating them from melting and alloying slags (Craddock, 1995, 203). However, in a  
292 Chalcolithic/Early Bronze Age context, copper smelting slag could also bear similar features of  
293 high copper content and mixed copper and iron oxides, due to locally highly varied redox  
294 conditions in a crucible or primitive furnace (Müller, et al., 2004, Burger, et al., 2010,  
295 Radivojevic, et al., 2010, Rehren, et al., 2016).

296 For the case of Taijiashi, it is less plausible if not impossible that primary smelting was  
297 conducted. A few relatively large scale copper smelting workshops of the Shang period have  
298 been identified in the Zhongtiao Mountain (Li, 2011), the Guanzhong Plains (Chen, et al., 2017),  
299 and the middle range of the Yangtze River Valley (Cui and Liu, 2017). Geographically, all these  
300 sites are located relatively close to major copper ore deposits. The analyses of their smelting  
301 slag show a copper content generally lower than 10 wt% (Li, 2011; Zou et al. in preparation,  
302 Zou, 2020). Given that copper smelting workshops had been established close to the mines, it  
303 makes little sense that ores were also brought to somewhere 200-300 km away for smelting.

304 Instead, a major part of Type II-b slag could be associated with refining. Three fourths of  
305 them have a copper content (combined metallic copper and copper oxide) higher than 10 wt%  
306 with an average of 20 wt% total copper reported as CuO. The elevated copper content serves  
307 as an indicator of refining since in such a less-controlled oxidizing process iron and copper can  
308 both turn into oxides (Tylecote, et al., 1977). Copper refining had previously been identified in  
309 workshops at Zhouyuan dated to the Western Zhou period (11<sup>th</sup>-8<sup>th</sup> century BC), based on the  
310 analyses of slag and raw copper found at the bronze foundries (Zhou, et al., 2009). The raw  
311 copper from those sites contains up to 9 wt% Fe and the refining slag is dominated by iron  
312 oxides and fayalite. Currently available analytical results of Shang period slag show no  
313 evidence of refining (Liang, et al., 2005, Huang, et al., 2011, Zhou, et al., 2015, Li, et al., 2018),  
314 even though analyses of bronze artefacts from the Late Shang period capital in Anyang have  
315 shown a trend of increasing iron content over time (Zhao, 2004). The ongoing investigation of  
316 the Middle Shang period copper smelting slag from the site of Tongling in Ruichang, Jiangxi  
317 province shows a significant iron content in embedded copper prills (frequently over 4 wt%)  
318 (Zou, 2020). The iron-rich raw copper therefore might have needed to be refined before alloying  
319 and casting.

320 About one-fourth of Type II-b slag fragments have a copper content of less than 10 wt%.

321 They could certainly be a product of varied redox conditions inside the refining vessel. An  
 322 alternative scenario is, however, also worth consideration. The recent investigation of the  
 323 Middle Shang Tongling site revealed a significant amount of mechanically crushed smelting  
 324 slag fragments (c. 0.5-1 cm in diameter), which are quite heterogeneous and typically rich in  
 325 magnetite (Figure 12) (Zou 2020; Zou et al. in preparation). Due to the chronological gap, the  
 326 Tongling site would not have been the copper source of Taijiasi, but it might reveal the general  
 327 features of Middle Shang copper smelting slag.

328

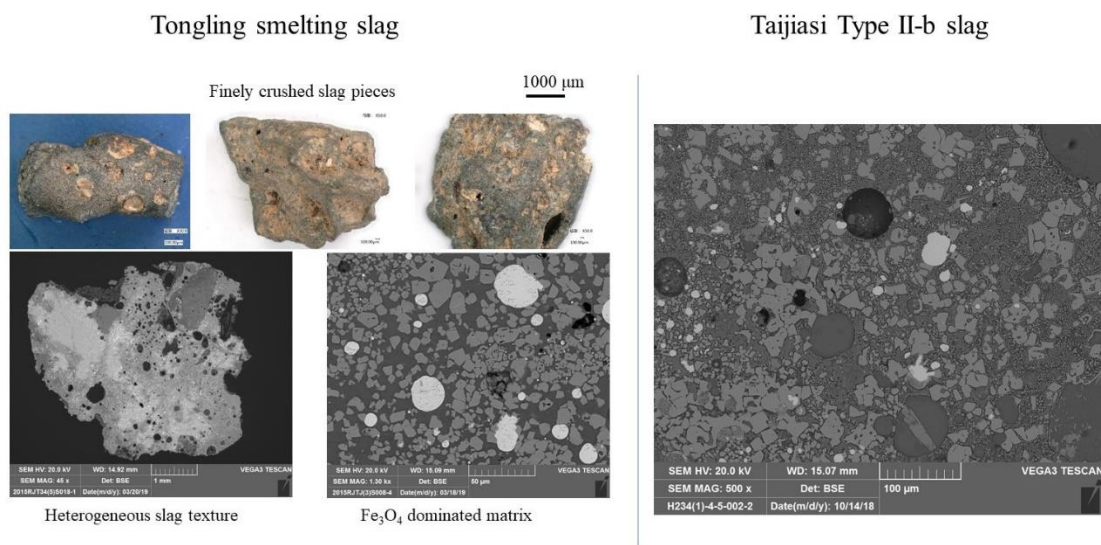


Figure 12 The comparison between Tongling and Taijiasi Type II-b slag. Their mineralogical compositions and heterogeneity are quite similar to each other.

329

330 The striking similarities between the Middle Shang smelting slag and Taijiasi Type II-b  
 331 slag drive us to think that some Type II-b slag could also be derived from crushing of smelting  
 332 slag (Figure 12). The heterogeneous nature of the smelting slag indicates it was quite viscous  
 333 and could trap copper easily. A preliminary mechanical processing at the smelting sites might  
 334 not be efficient enough in retrieving all copper prills, meanwhile leaving many copper lumps  
 335 containing still some adhering slag crumbs. These slag-copper composite pieces could have  
 336 been intentionally kept and shipped to the casting workshop for further cleaning and refining.  
 337 It was important to avoid them entering alloying/casting crucibles since their slag part was  
 338 difficult to melt ( $T > 1200\text{ }^{\circ}\text{C}$ ). The semi-solid slag fragments could cause metal loss or  
 339 compromise casting (e.g. by jamming the mould sprue). These composite fragments thus

340 needed to be first crushed, sorted, and even occasionally re-melted, leaving remains  
 341 mineralogically similar to smelting slag.

342 The copper processing activities at the site of Taijiasi are summarized as Figure 13. The  
 343 original materials could be iron-rich raw copper as well as a slag-copper composite from a  
 344 remote smelting site, and were refined at Taijiasi to relatively pure copper. The pure copper was  
 345 then mixed with fresh tin/tin oxide to make bronze and cast artefacts including ritual vessels,  
 346 weapons and many other items.

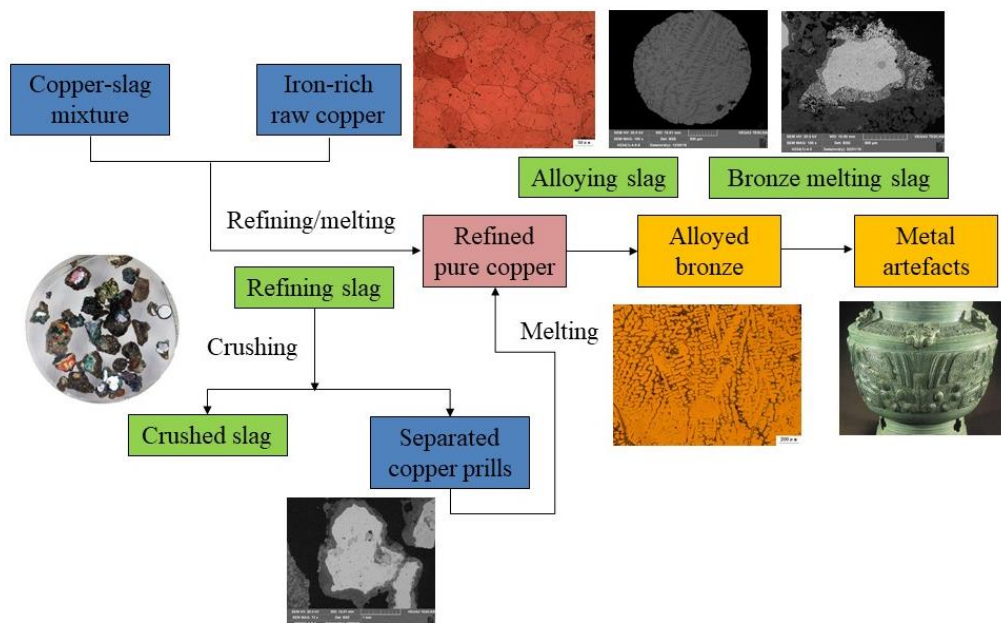


Figure 13 The reconstructed metallurgical *Chaîne opératoire* at the site of Taijiasi.

347

### 348 5. New perspectives in the study of Shang metallurgy

349 The micro-slag analysis does not only reveal the raw copper processing practices at Taijiasi,  
 350 but also indicated that most related slag remains were carefully collected and crushed before  
 351 being discarded within H234. It suggests that all activities of handling raw copper were  
 352 constrained to a single place, and all related slag was re-processed as much as possible until  
 353 down to quite fine fragments. In contrast, bronze alloying/casting slag was commonly found in  
 354 all areas of the site and apart from those in H234, they were discarded without much  
 355 reprocessing, as indicated by their size which is usually larger than 1 cm in diameter. The  
 356 presence of relatively iron-rich alloying/casting slag mostly in H234① strengthens this point.  
 357 It indicates that iron-rich raw copper was only available in H234 and could occasionally be

358 alloyed with tin without much refining. In other contexts, the copper used for making alloy had  
359 all been refined, most likely at H234. The location of H234 suggests it was probably under close  
360 supervision by people from the major buildings on the platform. The unalloyed copper is thus  
361 argued to be a strategic resource for the elite of this site and was not allowed to be accessed  
362 unsupervised. The alloying/casting slag, though rich in copper as well, was not collected for  
363 crushing, probably because the copper in them was mainly present in oxide form, making it  
364 much less accessible by physically processing. They were dumped with much less care and  
365 were more likely to be re-distributed to a much wider area of the site via secondary disturbances.

366 The question then arises whether workers from other Shang period sites conducted similar  
367 practices, or was what we saw at Taijiashi a local tradition of people living in the Huaihe River  
368 Valley. This is arguably an important new facet of investigation since it reflects people's varied  
369 attitudes to copper. Most likely, people who had better and easier access to copper resources  
370 would be less careful in terms of slag processing. So far, published analytical results of other  
371 Shang period metal workshops did not show evidence for copper refining and slag crushing  
372 practice. However, these were from privileged Central Plain sites, and since micro-slag samples  
373 were never actively collected from these sites, it is not yet possible to reach any meaningful  
374 conclusion regarding their management of this resource. More controlled excavations with  
375 careful sampling of micro-remains are much needed in future excavations of these sites.

376 Another important perspective is the provenancing of copper used during the Shang period.  
377 There have been decades of discussions surrounding the geological origin of copper, tin and  
378 lead in the Shang period (Jin, et al., 2017, Liu, et al., 2018a, Liu, et al., 2018b, Chen, et al.,  
379 2019 and references therein). Most previous discussions were based on elemental pattern and  
380 lead isotope ratios of finished artefacts, which contained a mixture of copper, lead and tin from  
381 various sources which would obviously render it more difficult pinpointing origins for each  
382 specific metal. Copper ingots were rarely found in Shang contexts and only a few of them have  
383 been analysed (Han and Ko, 2007, 221). Until now, though a number of Shang period copper  
384 mining and smelting sites have been identified, the geological origin(s) of much of the copper  
385 for Shang bronze is still not clear. While these copper mines mainly bear ores with common  
386 lead isotopic signatures ( $^{206}\text{Pb}/^{204}\text{Pb}<20$ ), their signature had been largely masked in artefacts  
387 containing highly radiogenic lead (Liu, et al., 2018b). The identification of refining slag at

388 Taijiasi offers a new hope to provenancing Shang copper, since the copper in the Type II slag  
389 was not yet alloyed and likely still preserves the geochemical features of its geological origin.  
390 Thus, these micro-slags are the best proxy in the Shang archaeological context for tracing the  
391 source(s) of copper supply. It is expected that in due course more refining slag will be identified  
392 in other Shang period bronze casting foundries, and cross-comparison of their isotopic data  
393 should shed new light on the discussion about the source and distribution network of copper in  
394 the Shang period.

395

### 396 **5.1 Invisible copper processing activities**

397 The detailed study of micro-slag from Taijiasi does not only enhance our understanding  
398 about Shang period metallurgy but also demonstrated the importance of micro-artefacts in the  
399 study of an ancient metallurgical workshop. Indeed, it has become common practice to carefully  
400 searching for hammer scale (iron oxide) with a magnet when excavating iron smithing  
401 workshops (e.g. Veldhuijzen and Rehren, 2007, Birch, et al., 2015, Lam, et al., 2018). However,  
402 a similar detailed sampling strategy has not yet been employed in the excavation of copper  
403 casting workshops. Commonly, lab-based researchers conducted their sampling on the  
404 metallurgical remains collected by excavators. These remains are typically large (>1cm in  
405 length/diameter) and bear metal corrosion or highly vitrified slaggy parts, making them readily  
406 identifiable in the field. However, considering the high value of copper, mechanical processing  
407 of copper smelting and refining/melting slag could arguably have been a common behaviour  
408 among early metallurgists. Without a careful excavation strategy, the potentially rich  
409 information retained in these micro-artefacts would have been lost.

410 The combination of pXRF survey, wet-sieving of soil samples and lab-based analysis has  
411 been shown to be an effective method for investigating a bronze casting workshop.  
412 Geochemical survey with pXRF can help excavators quickly locate interesting areas and loci  
413 based on their abnormally high concentration of copper, and has been utilized in many  
414 excavations of metallurgical workshops (Cook, et al., 2005, Cook, et al., 2010, Eliyahu-Behar,  
415 et al., 2012, Carey, et al., 2014) and even landscapes (e.g. Hanks, et al., 2015). However, little  
416 attention had been paid to the specific causes of these high readings. Various types of remains  
417 including ore and its tailings, slag, crucible lining, bronze prills, and corroding artefact

418 fragments could cause elevated copper content in soil. Identifying these different sources via  
419 detailed analyses could lead to quite different archaeometallurgical interpretations. Therefore,  
420 it is important in future excavations to collect copper-rich soil samples and study micro-  
421 artefacts in them, which would not only enhance our understanding about the metallurgical  
422 activities at workshop themselves but also provide a new facet for cross-comparative studies  
423 among varied workshops.

424

#### 425 Acknowledgements

426 We owe a lot of thanks to students and colleagues who participated in the field excavation of  
427 Taijiasi and the micro-slag sampling. We would like to particularly thank Professor Chen Bingbai  
428 of Wuhan University, the PI of the Taijiasi project. We thank Mr. Yan Bichen for conducting FTIR  
429 analyses of soil samples. We appreciate the precious advice from and discussion with Professor Lei  
430 Xingshan of Peking University and Professors Qian Wei and Chen Kunlong of USTB. This research  
431 is supported by the National Natural Science Foundation of China (No. 51704023, 51850410507),  
432 the National Social Science Foundation of China (No. 17ZDA178) and Fundamental Research  
433 Funds for the Central Universities (No. FRF-DF-19-007, No. FRF-TP-18-033A2).

434

435

436

#### 437 References

438 Berna, F., Behar, A., Shahack-Gross, R., Berg, J., Boaretto, E., Gilboa, A., Sharon, I., Shalev, S., Shilstein,  
439 S., Yahalom-Mack, N., Zorn, J.R., Weiner, S., 2007. Sediments exposed to high temperatures:  
440 reconstructing pyrotechnological processes in Late Bronze and Iron Age Strata at Tel Dor (Israel), *Journal*  
441 *of Archaeological Science* 34, 358-373.

442

443 Birch, T., Scholger, R., Walach, G., Stremke, F., Cech, B., 2015. Finding the invisible smelt: using  
444 experimental archaeology to critically evaluate fieldwork methods applied to bloomery iron production  
445 remains, *Archaeological and Anthropological Science* 7, 73-87.

446

447 Bourgarit, D., 2007. Chalcolithic copper smelting, in: La Niece, S., Hook, D., Craddock, P.T. (Eds.),  
448 *Metals and Mines: Studies in Archaeometallurgy*, Archetype Publications, London, pp. 3-14.

449

450 Burger, E., Bourgarit, D., Wattiaux, A., Fialin, M., 2010. The reconstruction of the first copper-smelting  
451 processes in Europe during the 4th and the 3rd millennium BC: where does the oxygen come from?,  
452 *Applied Physics A* 100, 713-724.

453

454 Carey, C.J., Wickstead, H.J., Juleff, G., Anderson, J.C., Barber, M.J., 2014. Geochemical survey and  
455 metalworking: analysis of chemical residues derived from experimental non-ferrous metallurgical

456 process in a reconstructed roundhouse, *Journal of Archaeological Science* 49, 383-397.

457

458 Chen, K., Liu, S., Li, Y., Mei, J., Shao, A., Yue, L., 2017. Evidence of arsenical copper smelting in Bronze  
459 Age China: A study of metallurgical slag from the Laoniupo site, central Shaanxi, *Journal of*  
460 *Archaeological Science* 82, 31-39.

461

462 Chen, K., Mei, J., Rehren, Th., Liu, S., Yang, W., Martínón-Torres, M., Zhao, C., Hirao, Y., Chen, J., Liu,  
463 Y., 2019. Hanzhong bronzes and highly radiogenic lead in Shang period China, *Journal of Archaeological*  
464 *Science* 101, 131-139.

465

466 Cook, S.R., Clarke, A.S., M.G., F., 2005. Soil geochemistry and detection of early Roman precious metal  
467 and copper alloy working at the Roman town of Calleva Atrebatum (Silchester, Hampshire, UK), *Journal*  
468 *of Archaeological Science* 32, 805-812.

469

470 Cook, S.R., Banerjea, R.Y., Marshall, L.-J., Fulford, M., Clarke, A., van Zwieten, C., 2010.  
471 Concentrations of copper, zinc and lead as indicators of hearth usage at the Roman town of Calleva  
472 Atrebatum (Silchester, Hampshire, UK), *Journal of Archaeological Science* 37, 871-879.

473

474 Craddock, P.T., 1995. *Early Metal Mining and Production*, Edinburgh University Press, Edinburgh.

475

476 Craddock, P.T., 2000. From hearth to furnace: Evidences for the earliest metal smelting technologies in  
477 the eastern Mediterranean, *Paléorient* 26, 151-165.

478

479 Cui, T., Liu, W., 2017. The new finds and research on the Tongling copper mining and smelting site in  
480 Ruichang, Jiangxi (江西瑞昌铜岭铜矿遗址新发现与初步研究), *Cultural Relics from South (南方文*  
481 *物)* 4, 57-63 (in Chinese).

482

483 Eliyahu-Behar, A., Yahalom-Mack, N., Shilstein, S., Zukerman, A., Shafer-Elliott, C., Maeir, A.M.,  
484 Boaretto, E., Finkelstein, I., Weiner, S., 2012. Iron and bronze production in Iron Age IIA Philistia: new  
485 evidence from Tell es-Safi/Gath, Israel, *Journal of Archaeological Science* 39, 255-267.

486

487 Epstein, S.M., 1993. *Cultural choice and technological consequences: Constraint of innovation in the*  
488 *late prehistoric copper smelting industry of Cerro Huaranga, Peru*, Unpublished PhD Thesis, University  
489 of Pennsylvania

490

491 Ge, J., 1959. Finding of Yin-Shang period bronze artefacts at Funan, Anhui province (安徽阜南发现殷  
492 商时代的青铜器), *Cultural Relics (文物)*, 2 (in Chinese).

493

494 Golden, J., Levy, T.E., Hauptmann, A., 2001. Recent discoveries concerning Chalcolithic metallurgy at  
495 Shiqmim, Israel, *Journal of Archaeological Science* 28, 951-963.

496

497 Han, R., Ko, T., 2007. *History of Science and Technology: Mining and Metallurgy (中国科学技术*  
498 *史·矿冶卷)*, Science Press (科学出版社) (in Chinese).

499



500 Hanks, B., Doonan, R.C.P., Pitman, D., Kupriyanova, E., Zdanovich, D., 2015. Eventful Deaths –  
501 Eventful Lives? Bronze Age Mortuary Practices in the Late Prehistoric Eurasian Steppes of Central  
502 Russia (2100-1500 BC), in: Renfrew, C., Boyd, M., Morley, I. (Eds.), *Death Rituals, Social Order and*  
503 *the Archaeology of Immortality in the Ancient World*, Cambridge University Press, Cambridge, pp. 328-  
504 347.

505

506 Hauptmann, A., 2014. The investigation of archaeometallurgical slag, in: Roberts, B.W., Thornton, C.P.  
507 (Eds.), *Archaeometallurgy in Global Perspective*, Springer, New York, Heidelberg, Dordrecht, London,  
508 pp. 91-105.

509

510 He, X., Gong, X., 2018. The excavation report of the Taijiashi site at Funan county, Anhui province (安徽  
511 阜南县台家寺遗址发掘简报), *Archaeology (考古)*, 3-13 (in Chinese).

512

513 Huang, J., Wei, G., Song, G., Li, S., Wang, C., 2011. Analyses on remains of smelting and casting copper  
514 at Xiaoshuangqiao site (小双桥遗址出土冶铸遗物的科技分析), *Nonferrous Metal (有色金属)* 63,  
515 147-152 (in Chinese).

516

517 Jin, Z.Y., Liu, R., Rawson, J., Pollard, A.M., 2017. Revisiting lead isotope data in Shang and Western  
518 Zhou bronzes, *Antiquity* 91, 1574-1587.

519

520 Lam, W., Chen, J., Chong, J., Lei, X., Tam, W.L., 2018. An iron production and exchange system at the  
521 center of the Western Han Empire: Scientific study of iron products and manufacturing remains from the  
522 Taicheng site complex, *Journal of Archaeological Science* 100, 88-101.

523

524 Li, J., 2011. Investigation and study on early copper mining and smelting sites in the south of Shanxi  
525 province, central China (晋南早期铜矿冶遗址考察研究), Unpublished PhD Thesis, University of  
526 Science and Technology Beijing (in Chinese)

527

528 Li, J., Li, Y., Tian, J., 2018. The study of metallurgical remains from the site of Dongxiafeng (东下冯遗  
529 址冶铸遗存研究), *Archaeology and Cultural Relics (考古与文物)*, 116-123 (in Chinese).

530

531 Liang, H., Li, Y., Sun, S., Tong, W., 2005. Analyses on As-containing slag unearthed from Shang Dynasty  
532 city site in Yuanqu country of Shanxi China (垣曲商城出土含砷渣块研究), *Nonferrous metals (有色*  
533 *金属)* 57, 127-130 (in Chinese).

534

535 Liu, R., Rawson, J., Pollard, A.M., 2018. Beyond ritual bronzes: identifying multiple sources of highly  
536 radiogenic lead across Chinese history, *Sci Rep* 8, 11770.

537

538 Liu, S., Rehren, Th., Pernicka, E., Hausleiter, A., 2015. Copper processing in the oases of northwest  
539 Arabia: technology, alloys and provenance, *Journal of Archaeological Science* 53, 492-503.

540

541 Liu, S., Chen, K.L., Rehren, Th., Mei, J.J., Chen, J.L., Liu, Y., Killick, D., 2018b. Did China Import  
542 Metals from Africa in the Bronze Age?, *Archaeometry* 60, 105-117.

543

544 Monnier, G.F., 2018. A review of infrared spectroscopy in microarchaeology: Methods, applications, and  
545 recent trends, *Journal of Archaeological Science: Reports* 18, 806-823.

546

547 Montero-Ruiz, I., 1993. Bronze Age metallurgy in southeast Spain, *Antiquity* 67, 46-57.

548

549 Müller, R., Rehren, Th., Rovira, S., 2004. Almizaraque and the Early Copper Metallurgy of Southeast  
550 Spain: New Data, *Madriider Mitteilungen* 45, 33-56.

551

552 Murillo-Barroso, M., Martínón-Torres, M., Massieu, D.C., Socas, D.M., González, F.M., 2017. Early  
553 metallurgy in SE Iberia. The workshop of Las Pilas (Mojácar, Almería, Spain), *Archaeol Anthropol Sci*  
554 9, 1539-1569.

555

556 O'Brien, W., 2004. Ross Island. Mining, Metal and Society in Early Ireland, National University of  
557 Ireland, Galway.

558

559 Rademakers, F.W., Rehren, Th., 2016. Seeing the forest for the trees: Assessing technological variability  
560 in ancient metallurgical crucible assemblages, *Journal of Archaeological Science: Reports* 7, 588-596.

561

562 Rademakers, F.W., Farci, C., 2018. Reconstructing bronze production technology from ancient crucible  
563 slag: experimental perspectives on tin oxide identification, *Journal of Archaeological Science: Reports*  
564 18, 343-355.

565

566 Radivojevic, M., Rehren, Th., Pernicka, E., Sljivar, D., Brauns, M., 2010. On the origins of extractive  
567 metallurgy: new evidence from Europe, *Journal of Archaeological Science* 37, 2775-2787.

568

569 Rehren, Th., 2003. Crucibles as reaction vessels in ancient metallurgy, in: Craddock, P.T., Lang, J. (Eds.),  
570 *Mining and Metal Production through the Ages*, Archetype, London, pp. 207-215.

571

572 Rehren, Th., Leshtakov, P., Penkova, P., 2016. Reconstructing Chalcolithic copper smelting at Akladi  
573 cheiri, Chernomorets, Bulgaria, in: Nikolov, V., Schier, W. (Eds.), *Der Schwarzmeerraum vom*  
574 *Neolithikum bis in die Früheisenzeit (6000-600 v.Chr.)*, Leidorf, Rhaden/Westfalen, pp. 205-214.

575

576 Rovira, S., 2002. Early slags and smelting by-products of copper metallurgy in Spain, in: Bartelheim, M.,  
577 Pernicka, E., Krause, R. (Eds.), *The Beginnings of Metallurgy in the Old World*, Verlag Marie Leidorf  
578 Rahden, Westf, pp. 83-98.

579

580 Shugar, A.N., 2003. Reconstructing the Chalcolithic metallurgical process at Abu Matar, Israel, in:  
581 *Proceedings of Archaeometallurgy in Europe I*, Milano, pp. 449-458.

582

583 Tylecote, R.F., Ghaznavi, H.A., Boydell, P.J., 1977. Partitioning of trace elements between the ores,  
584 fluxes, slags and metal during the smelting of copper, *Journal of Archaeological Science* 4, 305-333.

585

586 Veldhuijzen, H.A., Rehren, Th., 2007. Slags and the city: early iron production at Tell Hammeh, Jordan  
587 and Tel Beth-Shemesh, Israel, in: La Niece, S., Hook, D., Craddock, P.T. (Eds.), *Metals and Mines:*

588 Studies in Archaeometallurgy, Archetype Publications, London, pp. 189–201.  
589  
590 Zhao, C., 2004. Chemical analysis of bronze artefacts unearthed in Yinxu, Anyang (安阳殷墟出土青铜  
591 器的化学), Collected Papers on Archaeology (考古学集刊) 15, 243-268 (in Chinese).  
592  
593 Zhou, W., Chen, J., Lei, X., Xu, T., Chong, J., Wang, Z., 2009. Three Western Zhou bronze foundry sites  
594 in the Zhouyuan area, Shaanxi province, China, in: Mei, J., Rehren, Th. (Eds.), Metallurgy and  
595 Civilisation: Eurasia and Beyond, Archetype, London, pp. 62-72.  
596  
597 Zhou, W., Liu, Y., Yue, Z., 2015. Scientific study on two types of copper processing containers from the  
598 Xiaomintun site in Anyang (安阳殷墟孝民屯出土两类熔铜器具的科学研究), Cultural Relics from  
599 South (南方文物), 48-57 (in Chinese).  
600  
601 Zou, G., 2020. Archaeometallurgical Investigation of the Tongling Site at Ruichang in Jiangxi Province  
602 (江西瑞昌铜铃遗址商代冶金考古综合性研究), Unpublished PhD Thesis, University of Science and  
603 Technology Beijing (in Chinese)  
604  
605